

## A physical–biogeochemical coupling scheme for modeling marine coastal ecosystems

Ramón Filgueira<sup>a, b, \*</sup>, Jon Grant<sup>b</sup>, Cédric Bacher<sup>c</sup>, Michel Carreau<sup>d</sup>

<sup>a</sup> Consejo Superior de Investigaciones Científicas (CSIC), Instituto de Investigaciones Marinas, c/Eduardo Cabello 6, 36208 Vigo, Spain

<sup>b</sup> Department of Oceanography, Dalhousie University, Halifax, Canada NS B3H 4J1

<sup>c</sup> French Institute for Sea Research (IFREMER), BP70, 29280 Plouzané, France

<sup>d</sup> Hatch Ltd, 5 Place Ville Marie Suite 200, Montréal, Québec, Canada H3B 2G2

\*Corresponding author : Ramón Filgueira, email address : [ramonf@iim.csic.es](mailto:ramonf@iim.csic.es)

### Abstract:

Ecological modeling of dynamic systems such as marine environments may require detailed spatial resolution when the modeled area is greatly influenced by complex physical circulation. Therefore, the simulation of a marine ecosystem must be underlain by a physical model. However, coupling hydrodynamic and biogeochemical models is not straightforward. This paper presents a modeling technique that can be used to build generic and flexible fully-spatial physical–biogeochemical models to study coastal marine ecosystems using a visual modeling environment (VME). The model core is constructed in Simile, a VME that has the capacity to create multiple instances of submodels that can be interconnected, producing a fully-spatial simulation. The core is designed to assimilate a choice of different hydrodynamic models by means of matrices, enhancing its compatibility with different software. The biogeochemical model can be modified by means of a graphical interface, which facilitates sharing within the scientific community. This paper demonstrates the application of the coupling scheme to mussel aquaculture in Tracadie Bay (PEI, Eastern Canada). The model was run for two different years, 1998 and 1999, and indicated that mussel biomass exerts a top-down control of phytoplankton populations, causing a maximum chlorophyll depletion of 61.0% and 80.3% for 1998 and 1999 respectively. The difference between both years highlights the importance of inter-annual variability, which is significant from an ecosystem-level perspective because it reveals the relevance of applying a precautionary policy in the management of aquaculture activity. Therefore, the proposed core developed in Simile is a generic and flexible tool for modeling long-term processes in coastal waters, which is able to assimilate a choice of hydrodynamic models, constituting a novel approach for generating fully-spatial models using visual modeling environments.

### Highlights

► An offline physical–biogeochemical coupling scheme for marine systems is presented. ► The scheme can be used as a generic core to create fully-spatial models. ► The biogeochemical model can be easily modified using the Simile's GUI. ► Its application is demonstrated in an aquaculture site in PEI (Eastern Canada).

**Keywords:** Physical–biogeochemical coupling; Marine spatial planning; Aquaculture; Simile

37

38 **1. Introduction**

39 Dynamic ecosystem models provide a powerful approach to predict the consequences of  
40 natural or anthropogenic changes related to pollution, climate change, land-use patterns and  
41 other impacts. Models of marine ecosystems contain many examples of successful  
42 application of this approach, including nutrients cycles, contaminant dispersion,  
43 eutrophication and aquaculture-ecosystem interactions (e.g., Sarmiento et al., 1993; Chapelle  
44 et al., 1994; Baretta et al., 1995; Allen et al., 2010; Filgueira and Grant, 2009; Grant and  
45 Filgueira, in press). Ecosystem models have been used in the field of shellfish aquaculture to  
46 evaluate how the energy flow toward cultured biomass may potentially alter the food supply  
47 for other trophic levels such as natural benthos (Cloern, 1982; Dowd, 2003). In addition,  
48 ecological modelling is valuable in the study of bivalve growth and/or culture carrying  
49 capacity (Bacher et al., 1998; Dowd, 1997; Duarte et al., 2003; Ferreira et al., 1998; Grant et  
50 al., 2007a; Pastres et al., 2001; Raillard and Menesguen, 1994) and the effects of aquaculture  
51 on the ecosystem (Chapelle et al., 2000; Dowd, 2005). Carrying capacity models have been  
52 applied to manage cultivation areas (Bacher et al., 1998; Duarte et al., 2003; Ferreira et al.,  
53 1998) or increase profit in new areas (Heral, 1993). Given that coastal ecosystems are  
54 influenced largely by hydrodynamics, dynamic fully-spatial models must be underlain by a  
55 hydrodynamic model including the influence of diffusion–advection forced by tides, winds,  
56 and density gradients.

57

58 Circulation is the spatial manifestation of these processes and division of the environment  
59 into grid cells (e.g. finite element grid) allows these flows to be spatially resolved. The grid  
60 cells are not only connected, but they are conservative with respect to water flux, requiring a

61 hydrodynamic model based on equations of water motion. Although the models can be  
62 simplified, as in tidal prism calculations, spatial resolution is also sacrificed. There are many  
63 examples in which a hydrodynamic model is integrated with ecosystem fluxes to create  
64 spatial simulations (e.g. Ferreira et al., 2008; North et al., 2010), but this integration is not  
65 straightforward. For example, visual modelling environment (VME) software such as Stella  
66 (<http://www.iseesystems.com>) allows users to create models without writing code  
67 (Muetzelfeldt and Massheder, 2003). This has many advantages such as increased availability  
68 of simulation tools to non-specialists (i.e. researchers without in-depth knowledge of  
69 informatics/code programming), sharing of models between users, and efficient re-use of  
70 submodels (Silvert, 1993). Despite the sophistication of some VMEs, the ability to  
71 incorporate spatial realism as well as hydrodynamics has been limited and according to our  
72 knowledge there are no studies in the literature in which VMEs were used to generate  
73 detailed spatial resolution models of dynamic systems such as marine environments. VMEs  
74 have been more successfully applied to terrestrial environments (e.g. Elshorbagy et al., 2006;  
75 Randhir and Tsvetkova, 2011) in which physical processes such as groundwater flow can be  
76 simplified relatively easily compared to coastal hydrodynamics. For marine environments,  
77 improved ability to easily construct coupled physical-biogeochemical fully-spatial models  
78 based on VME would be beneficial, because it is a natural extension of the spatial context  
79 fostered by GIS, marine spatial planning and ecosystem-based management.

80

81 In addition, although the examples cited above are well-developed marine ecosystem models,  
82 the methodology is not easily adapted to other locations. Our focus in this paper is to provide  
83 insight about the integration of biogeochemical and ecological data with circulation models  
84 using object-oriented software, and to deliver a generic and flexible coupling environment

85 where the effort to export the model to other locations is reduced. The coupling scheme is  
86 developed in Simile (Appendix A), which is well suited to spatial models because it allows  
87 ‘multiple instances’ of a given submodel that can be interconnected, creating spatial  
88 connections (Muetzelfeldt and Massheder, 2003). In this study we demonstrate the  
89 application of the coupling scheme with an example from an aquaculture site in Prince  
90 Edward Island (Eastern Canada). In this example we used AquaDyn to create the  
91 hydrodynamic model and Matlab to calculate and deliver water exchange coefficients into  
92 Simile. We emphasize that AquaDyn and Matlab are not specific requirements of the  
93 coupling scheme, they are the tools used in this specific example. Other hydrodynamic  
94 models such as open source FVCOM (<http://fvcom.smast.umassd.edu/>) can also be used, as  
95 well as the open source Octave (<http://www.gnu.org/software/octave/>), R ([http://www.r-](http://www.r-project.org/)  
96 [project.org/](http://www.r-project.org/)) or Scilab (<http://www.scilab.org/>) instead of Matlab  
97 (<http://www.mathworks.com/>).

98  
99

## 100 **2. Material and Methods**

### 101 ***2.1. Description of the physical-biogeochemical coupling scheme***

102 In detailed spatial resolution models software must keep track of spatial locations and be  
103 suited to mapping, which is not generally a feature of VME applications. Fully-spatial models  
104 require more spatial complexity than the few boxes that can easily be set up in commercially-  
105 available VMEs. However, Simile is highly adaptable to handling spatial information, but  
106 there may be similar capacity in other software. Simile allows ‘multiple instances’ of a  
107 submodel that can represent the topology of the finite element grid created by the  
108 hydrodynamic model. These finite element grids are commonly composed by triangles or

109 squares called elements, which are defined by nodes and links (Figure 1a). The  
110 hydrodynamic model reports water velocity and direction for each node, allowing a  
111 calculation of water exchange between elements, which accounts for the hydrodynamics of  
112 the spatial connections. The crux of the coupling scheme is as follows (Figure 2):

- 113 • The hydrodynamic model generates a finite element grid and corresponding  
114 hydrodynamic regime.
- 115 • Simile reads the spatial topology of the finite element grid and hydrodynamics, which  
116 allow the coupling with the biogeochemical model.
- 117 • The biogeochemical results from Simile track the spatial topology, which can then be  
118 exported to GIS.

119

## 120 *2.2. Adapting hydrodynamic results to Simile*

121 The steps described in this section are common to all hydrodynamic models that can deliver  
122 results organized in matrices such as AquaDyn (Appendix A) or FVCOM. The following  
123 procedures (See Appendix B for a detailed description) were automated through a Matlab  
124 script:

- 125 • Velocity vectors are combined as root mean square velocities across grid boundaries  
126 to calculate the water flux in each element link for each time step. It is recommended  
127 the smallest time step possible be combined with the available computational power  
128 in order to provide the best resolution to the time series.
- 129 • Water fluxes of each time step are combined to generate average volumetric water  
130 exchange for each link.
- 131 • An optimization algorithm is applied to minimize the potential residual water  
132 imbalance caused by the averaging procedure.

133 • A matrix is generated with the averaged volumetric water exchange for each link.

134

135 We present an example using averaged hydrodynamics rather than time-dependent flows in  
136 order to simplify the coupling scheme. The volumetric water exchange between elements is  
137 calculated simultaneously in the whole grid following a first order upwind scheme. The water  
138 exchange between two adjacent elements is not calculated as a net flow but as a dispersion  
139 flow. This is a generalization of the tidal prism method at the scale of each element such that  
140 for each link between two adjacent elements, two averaged flows are calculated, one going  
141 from element  $i$  to  $j$  and one going from  $j$  to  $i$ . These exchange coefficients are divided by the  
142 volume of the elements where the flow enters in order to provide rates expressed as  
143 percentage day<sup>-1</sup>.

144

### 145 ***2.3. Simile structure to read spatial information***

146 Simile establishes relationships between the different submodels, which represent the  
147 elements of the grid, using its ‘Condition’ function, which specifies whether a connection  
148 between submodel instances exists. The use of ‘Condition’ requires a specific submodel that  
149 is described in Appendix C. This submodel allows reading the topology and the  
150 hydrodynamics of the hydrodynamic model by means of matrices. Therefore, this submodel  
151 provides a template that can be used as a core to develop any physical-biogeochemical model  
152 in Simile without further altering the coupling scheme itself.

153

154 In order to verify that water exchange parameterized within Simile is consistent with the  
155 physics predicted by the hydrodynamic model, a simple verification process is suggested.

156 Both Simile and the hydrodynamic model are set up in the same way to run a model in which

157 a conservative tracer is the only component. Assuming a constant concentration of the tracer  
158 at the boundary and a lower and homogeneous distribution inside the bay at time 0, the model  
159 is run until equilibrium is reached. By comparing the tracer distribution in the bay after a  
160 period of time, we determine if Simile is correctly assimilating the hydrodynamics. It is very  
161 important to compare the general pattern and not the high frequency events, because the  
162 hydrodynamic model is using a continuous time series of water exchange and depth,  
163 including tidal variation, while Simile is using averaged values. This verification procedure is  
164 an internal control of the coupling process and does not exempt the researcher from  
165 validation of the physical and biogeochemical model.

166

#### 167 ***2.4. Exporting the results to GIS***

168 Simile outputs provide a single value for each triangular element, but these triangles are  
169 differently sized. Therefore, if these data were plotted in GIS, the weighting represented by  
170 the area of the triangle would not be preserved. This can be corrected by calculating the  
171 position of geometric reference points (Figure 1) within each triangle (Script available on  
172 request) based on its geometry:

- 173 • Centroid: the point of intersection of triangle medians (the lines joining each vertex  
174 with the midpoint of the opposite side). The centroid is the center of mass of an  
175 element and therefore the single value output by Simile.
- 176 • Nodes: the triangle's vertices calculated as the average of the centroids sharing the  
177 same vertex.
- 178 • Midpoints between the centroid and each node: calculated as the average between the  
179 centroid and the corresponding vertex.

180

181 These geometric points provide a grid that accounts for the differential area of grid cells. The  
182 maps we show below (Figure 4 and 10) were created with this method and plotted using  
183 AquaDyn capabilities. In addition, the Cartesian coordinates used in the hydrodynamic model  
184 may be normalized to UTM and used in any GIS.

185

## 186 ***2.5. Tracadie Bay Example***

### 187 ***2.5.1. Study Site and objective***

188 An example of the coupling approach is presented for Tracadie Bay, Prince Edward Island,  
189 Canada (Figure 3). The bay is a small ( $16.4 \text{ km}^2$  at mean tide and  $13.8 \text{ km}^2$  at low tide),  
190 shallow (maximum depth 6 m) barrier beach inlet with semidiurnal tides (range of 0.6 m). It  
191 is open to the Gulf of Saint Lawrence through a single narrow channel. Exchange of the bay  
192 with the offshore is up to  $500 \text{ m}^3 \text{ s}^{-1}$  (Dowd, 2003), which results in a turnover of the entire  
193 volume of the Bay every 4-10 days (Dowd, 2005). Winter Harbour empties into the southeast  
194 of Tracadie Bay where Winter River drains a large watershed, but the input of freshwater is  
195 low for much of the year ( $\sim 1 \text{ m}^3 \text{ s}^{-1}$ ; see also Cranford et al., 2007). Mussel culture in the bay  
196 is located as shown in Figure 3 and the biomass calculated according to Dowd (2003, 2005),  
197 who estimated a standing stock of between 1 and  $2 \times 10^6$  kg wet weight mussels. The  
198 standing stock of  $1.5 \times 10^6$  kg wet weight of mussels is considered the actual scenario in  
199 Tracadie Bay and it is homogeneously distributed in culture areas (Figure 3). Tissue weight  
200 was calculated assuming a condition index of 30%. Dry weight was calculated assuming  
201 water content of 80% and a carbon content of 40% mussel dry weight.

202

203 The goal of this example is to analyze phytoplankton depletion due to suspension feeding  
204 contrasting two consecutive years, 1998 and 1999, with different far-field conditions, and to



205 demonstrate the potential of the model for studying the implications of inter-annual variations  
206 in carrying capacity estimations. The main purpose of this example is to show how to apply  
207 the coupling scheme. Implications of the model for aquaculture environment interactions  
208 have been explored in the references cited below.

209

### 210 ***2.5.2. Hydrodynamic Model***

211 The boundaries and depths of the bay were digitized from a hydrographic chart. The finite  
212 element mesh was generated within AquaDyn, tuning mesh size and density. The 2D  
213 hydrodynamics was forced by a time series of sea level, and friction was applied via a  
214 Manning coefficient. The resulting triangular mesh contained 544 elements, and 1454  
215 connections across links. Application of an AquaDyn model to Tracadie Bay was validated  
216 using sea level data (Grant et al., 2005). In the present study, the hydrodynamic model was  
217 further ground-truthed by comparing the modulus of velocity vector in Node # 236 with  
218 current meter time series available for the same location (46°23'56''N, 62°59'56''W) and  
219 period between 15 June and 15 September 2002.

220

### 221 ***2.5.3. Biogeochemical model***

222 The biogeochemical model used in Simile is based on a classical PNZ model (phytoplankton  
223 (P) – Nutrients (N) – Zooplankton (Z)) with the addition of mussel (M) and detritus (D)  
224 submodels. Given the minimal effect of Zooplankton in the results, this submodel was turned  
225 off in subsequent scenarios. All the submodels are characterized in terms of carbon per cubic  
226 meter ( $\text{mg C m}^{-3}$ ), with the exception of dissolved nutrients, which are expressed as  
227 milligrams of nitrogen per cubic meter ( $\text{mg N m}^{-3}$ ). The equations of the model are based on  
228 Kremer and Nixon (1978), a brief description of the different terms is given in Table 1 and a

229 detailed description as well as the exact values of the parameters are given in Grant et al.  
 230 (1993, 2007a, 2008), Dowd (1997, 2005) and Filgueira and Grant (2009). The differential  
 231 equations are as follows:

$$232 \quad \frac{dP}{dt} = +P_{growth} - P_{mortality} - M_{grazing} \pm P_{mixing} \quad \text{Eq. 1}$$

$$233 \quad \frac{dN}{dt} = +N_{river} + M_{excretion} - P_{uptake} \pm N_{mixing} \quad \text{Eq. 2}$$

$$234 \quad \frac{dD}{dt} = +D_{resuspension} + M_{feces} + P_{mortality} - D_{sinking} - M_{grazing} \pm D_{mixing} \quad \text{Eq. 3}$$

$$235 \quad \frac{dM}{dt} = +M_{net\ growth} + M_{seeding} - M_{mortality} - M_{harvesting} = 0 \quad \text{Eq. 4}$$

236 The mussel compartment biomass is assumed to be constant over time, so that the mussel  
 237 biomass interacts with the ecosystem model as a forcing function rather than a response  
 238 variable (Dowd, 2005). By manipulating forcing by mussel biomass, some of the more  
 239 uncertain steps related to aquaculture activity are not required (for example, farming  
 240 processes like harvesting and seeding, or bivalve size distribution). In addition, bivalve  
 241 mortality rate is not explicit in the model. In essence, this assumption means that the growth  
 242 of the bivalves and seeding activity is compensated by mortality rate and harvesting,  
 243 providing the constant biomass.

244

245 The model was run between 15 June and 15 September for two years, 1998 and 1999. The  
 246 main differences between both years are related to suspended detritus content and wind  
 247 speed. Average organic detritus content of  $857 \pm 250 \text{ mg C m}^{-3}$  and  $565 \pm 193 \text{ mg C m}^{-3}$  was  
 248 observed in 1998 and 1999, respectively. In addition, the percentage of days with wind  
 249 speeds higher than  $5 \text{ m s}^{-1}$ , the threshold for bottom resuspension (Filgueira and Grant, 2009;  
 250 Walker and Grant, 2009), was 8.89 % and 2.22 % in 1998 and 1999, respectively. Waite et al.

251 (2005) and Filgueira and Grant (2009) provide further details of the model as well as the  
252 boundary conditions.

253

254 Ground-truthing was carried out by comparing the modelled chlorophyll values in Element #  
255 182 (See Figure 3 for location) with observations in both years, 1998 and 1999. The time  
256 series were analyzed with major axis regression method (RMA) following Duarte et al.  
257 (2003). The significance of the regression was tested using ANOVA and comparison of the  
258 slope and intercept with 1 and 0, respectively, carried out following Zar (1984).

259

260

### 261 **3. Results**

#### 262 **3.1. Ground-truthing**

263 The average measured water speed values and standard deviation were higher than the  
264 modelled values (Table 2), because current meter dataset contains extreme values, caused by  
265 strong local winds, which exert a bias in the time series comparison. A better indicator of  
266 central tendency for skewed distributions is the median, which minimizes the contribution of  
267 extreme values and outliers. Median values of the model,  $4.18 \text{ cm s}^{-1}$ , were in good  
268 agreement with the current meter values,  $4.48 \text{ cm s}^{-1}$ , suggesting that the circulation model  
269 realistically reproduced the hydrodynamics.

270

271 The calculation of the first order upwind scheme error (Appendix B) in the chlorophyll  
272 compartment resulted in an averaged value over the elements and time of 0.029% (maximum  
273 1.005%) and 0.097% (maximum 1.738%) respectively, which is an excellent indication that  
274 cell size and daily averaging time step are small enough. In addition, the verification test

275 described (Section 2.3) was performed in order to verify that Simile is correctly assimilating  
276 the hydrodynamics from AquaDyn. Both models were set up with a constant tracer  
277 concentration in the boundary of 2 units  $\text{m}^{-3}$  and an initial tracer concentration in the domain  
278 of 1 unit  $\text{m}^{-3}$ . The distribution of the tracer after 10 days (Figure 4) shows a similar pattern in  
279 both AquaDyn and Simile. The largest discrepancies between both approaches are located in  
280 the northeastern part of the bay. Two elements (See Figure 3 for location) were analyzed in  
281 detail for a longer period of time, one located in the northeastern part of the bay (element  
282 385) and another located in the southern section (element 182). Original AquaDyn time series  
283 were transformed by applying a moving average regression in order to smooth high  
284 frequency events with a period lower than one day (e.g. wind and tides), in order to provide  
285 an average value for each day (Figure 5). This analysis highlights the better agreement in the  
286 southern section, element 182. However, the discrepancies between AquaDyn and Simile in  
287 the northern section, element 385, become smaller with time. Although the tracer is slightly  
288 different in this element after 30 days, this convergence pattern and the similar spatial  
289 distribution indicate that Simile is properly assimilating the AquaDyn output of the  
290 hydrodynamics.

291

292 Ground-truthing of the coupled physical-biogeochemical model was carried out by  
293 comparing modelled and observed values of chlorophyll. The ANOVAs indicated that the  
294 regressions (1998:  $\text{Modelled} = 1.13 \pm 0.14 \text{ Observed} + 11.95 \pm 17.14$ ,  $r^2 = 0.47$ ,  $p < 0.05$ ; 1999:  
295  $\text{Modelled} = 0.85 \pm 0.09 \text{ Observed} + 36.34 \pm 25.78$ ,  $r^2 = 0.52$ ,  $p < 0.05$ ) are statistically significant.  
296 Analysis of the slopes showed that in 1998 the model follows the same pattern as the  
297 observations ( $p = 0.356$ ). However, in 1999 the slope was less than 1 ( $p < 0.05$ ), indicating that

298 the results of the model are offset from the observations. The intercepts are greater than 0  
299 indicating that the model is slightly enriched in chlorophyll compared to the observed values.

300

### 301 **3.2. Model results**

302 The physical-biogeochemical model was run between 15 June and 15 September in two  
303 scenarios for each year (1998 and 1999): without mussels and with a mussel standing stock of  
304  $1 \times 10^6$  kg wet weight, the minimum biomass in Tracadie Bay according to previous studies  
305 (Dowd, 2003, 2005). Model outputs are shown as the percentage of chlorophyll depletion in  
306 the mussel scenarios compared to the non-mussel scenario. The bay-averaged chlorophyll  
307 depletion over the studied period ranged from 4.8% to 44.4% and 10.3% to 58.6% in 1998  
308 and 1999, respectively (Figure 6). The maximum daily depletion observed in an element in  
309 the bay was 61.0% and 80.3% for 1998 and 1999, respectively. The time-averaged  
310 chlorophyll depletion for the whole bay was  $26.6 \pm 8.1\%$  and  $30.0 \pm 8.8\%$  for 1998 and 1999,  
311 respectively. These differences are caused by the variation in boundary forcing conditions  
312 between years. The time-averaged chlorophyll depletion (Figure 7) is related to the culture  
313 area displaying decreases in depletion in the direction of nutrient sources, i.e. toward Winter  
314 River and the inlet (Gulf Saint Lawrence), where culture density is negligible. In addition, the  
315 effect of different boundary conditions between years can be observed, showing more intense  
316 and extended chlorophyll depletion in 1999 compared to 1998.

317

318

## 319 **4. Discussion**

320 The ability to couple physical and biogeochemical models is fundamental to simulating  
321 marine ecosystems. These coupling schemes can be classified as 'integration', 'online

322 coupling' and 'offline coupling'. Integration refers to utilizing physical exchange in a  
323 reduced spatial resolution, e.g. rates averaged across space for a box model. At the other end  
324 of the linkage spectrum between physics and biogeochemistry, online coupling indicates that  
325 both physical and biogeochemical models run simultaneously. In between are offline  
326 coupling techniques, where the physics is run first and the biogeochemical model is run  
327 subsequently using physical outputs at different time steps but the same spatial scale. Fully  
328 spatial models constructed in VMEs require offline coupling given the limited connectivity  
329 with physical simulation software. Our motivation in the present study is to provide insight  
330 into the integration of physical and ecological data using a visual modelling environment  
331 (VME), which, to our knowledge, is the first example in the literature in which a VME is  
332 used to generate a fully spatial model.

333

334 There are other approaches in the literature (Table 3) that usually require expertise in  
335 language programming and/or specific sophisticated software to create/modify modules, and  
336 in some cases the structure of these modules is rigid and non-modifiable. The coupling  
337 scheme described in this paper represents a novel approach to create fully-spatial models  
338 using a Visual Modelling Environments (VME). VMEs such as Stella or Simile have  
339 commonly been used in scientific literature given their smooth learning curve. VMEs are  
340 based in objects that represent stocks, flows, variables and their interactions. The connections  
341 of these objects symbolize ecological processes, and the fact that they can be visualized  
342 facilitates access to non-programmers. These visual symbols make it easier to spread and  
343 share models in the scientific community, a cornerstone for improving the conceptual design  
344 of any model.

345

346 The general scheme described in this paper constitutes a generic and flexible core for  
347 coupling physical-biogeochemical models in coastal areas. The specifics of the ecosystem  
348 model are initially developed in Simile and the submodels described in this paper allow the  
349 coupling of hydrodynamics constructed in a different modelling environment, which can be  
350 2D or 3D. In fact, the described scheme is quite flexible and can be used with only a few cells  
351 to construct a box model. When the coupling scheme is applied to a new site, the  
352 biogeochemical model can be re-used and the principal effort is focused on the hydrodynamic  
353 model. Once the model is developed, the results can be exported to GIS for mapping,  
354 increasing the connectivity of the model with other applications. Another advantage of the  
355 coupling scheme developed in Simile is that the optimization tool PEST (Model-Independent  
356 Parameter ESTimation, Watermark Numerical Computing) is integrated into Simile. PEST  
357 can be used with two objectives in mind: (1) tune parameters in order to calibrate the model,  
358 avoiding “eyeball” calibrations, or with the appropriate dataset estimates unknown or  
359 uncertain parameters, and (2) optimize management strategies according to a variety of  
360 criteria (e.g. Filgueira et al., 2010).

361

362 The coupling technique used in Simile follows an offline unidirectional scheme, that is, the  
363 hydrodynamic model is run first and the results are delivered to the biogeochemical model  
364 that is run subsequently, without providing feedback to the hydrodynamic model. This is not  
365 a problem in this particular case given that the feedback of the biogeochemical model is not  
366 relevant for the hydrodynamics of the bay. In fact, in shallow waters, tides, winds and  
367 freshwater, runoff drives components of the circulation (Kjerfve and Magill, 1989). The  
368 hydrodynamics are averaged following a first-order upwind scheme before being delivered to  
369 the biogeochemical model. Since this averaging process dilutes the effect of high frequency

370 events, the application of the model scheme is limited to the study of long-term processes.  
371 These aspects of offline coupling must be taken into account when the general goals are set.  
372  
373 The described coupling scheme was applied to Tracadie Bay, a shallow bay with extensive  
374 aquaculture activity. This application is presented as an example of the coupling scheme and  
375 not as a research exercise itself. The bay is an excellent test bed because we have conducted a  
376 variety of field and modelling studies there. Grant et al. (2008) employed a model of seston  
377 depletion in Tracadie Bay in which AquaDyn results were coupled with a Matlab ecosystem  
378 model. Although specific to average seasonal nutrient, temperature, and boundary conditions,  
379 maps of seston depletion (Figure 4B in Grant et al., 2008) show near-identical patterns to  
380 those depicted in Figure 7. In addition, the chlorophyll depletion values of 61.0% and 80.3%  
381 for 1998 and 1999, respectively, are in good agreement with the values observed by Grant et  
382 al. (2007b, 2008) in the same bay during a short-term experiment. These authors predicted a  
383 67% reduction in chlorophyll in the north-south transect of Tracadie bay, the main axis of the  
384 bay where mussel culture is located.

385  
386 The approaches to shellfish aquaculture models can be divided into box models and fully-  
387 spatial physical-biogeochemical models (Grant and Filgueira, in press). Although it is  
388 possible to simplify hydrodynamics and include them in a box model, the spatial detail  
389 provided by a fully-spatial physical-biogeochemical model is desirable for two reasons. (1)  
390 high spatial resolution allows us to simulate the effects of farm location on the ecosystem and  
391 the interaction between farms (e.g. Figure 7). Therefore, management policies related to  
392 spatial arrangement of farms can be pursued as well as a prediction of bivalve growth rate as  
393 a function of culture biomass in each location. (2) The results can be mapped, an obvious



394 advantage for representing trends and gradients in marine systems. Spatial resolution can also  
395 affect the results of the model, especially when processes are dependent on concentration  
396 (Fennel and Neumann, 2004).

397

398 In conclusion, we have focused on Simile, which incorporates a graphical user interface, is an  
399 object-oriented software, and offers the capability of topology recognition using matrices, an  
400 ideal modelling platform from which to pursue physical-biogeochemical simulation. The  
401 coupling scheme has satisfied tests of internal and external consistency and conservative  
402 behavior, and shown results compatible with previous field and modelling studies of the test  
403 location. The Simile coupling scheme has the following positive characteristics: (1) the  
404 biogeochemical model can be modified by way of a user-friendly graphical interface; (2)  
405 knowledge of programming language is minimized; (3) results can be exported to GIS, and  
406 (4) an optimization tool (PEST) is integrated. Therefore, the proposed core developed in  
407 Simile is a generic and flexible tool for modelling long-term processes in coastal waters,  
408 which is able to assimilate a choice of hydrodynamic models, constituting a novel approach  
409 for generating fully-spatial models using visual modelling environments.

410

411

#### 412 **Acknowledgements**

413 This research was funded by a Strategic Project Grant and Discovery Grant from the Natural  
414 Sciences and Engineering Research Council of Canada (NSERC) to JG. RF salary was  
415 supported by an Angeles Alvariño (Xunta de Galicia) contract and a Xunta de Galicia  
416 fellowship co-funded by the European Social Fund (Operative Program Galicia 2007-2013).

417 **Appendix A. Software description**

418 Simile is a graphical system-dynamics modelling tool that incorporates object-oriented  
419 concepts. The software is available from Simulistics Ltd. Visit <http://www.simulistics.com> or  
420 email [info@simulistics.com](mailto:info@simulistics.com) for details. Simile is available for Windows (95 onwards), Linux  
421 (all) and MacOS (OSX 10.3 onwards). It takes between 20 and 50 MB of disk space  
422 depending on the platform. Simile has a proprietary license but its data formats are open.  
423 Models can be freely distributed, and those built with Simile Enterprise can be run on a free  
424 version of the software.

425

426 AquaDyn is a two dimensional free surface water hydrodynamic and dispersion software that  
427 uses a finite element technique to solve the St-Venant equations. AquaDyn takes into account  
428 bathymetry, bed friction, wind stress, turbulent dissipation and complex coastlines. The  
429 software can be obtained from Hatch Ltd. Email or call Michel Carreau ([mcarreau@hatch.ca](mailto:mcarreau@hatch.ca);  
430 +1 514-864-5500 (ext. 6108)) for further details. The entire package once installed takes less  
431 than 10 megabytes of space. Each model within AquaDyn is stored within one project file  
432 which contains all inputs and outputs; the file size is typically smaller than 3 megabytes. The  
433 software executable has been available since 1995 (the source code is not available for  
434 distribution) and can be run on any Windows 32 bits operating system.

435

436 In addition to the validation performed by the developers, AquaDyn has been used and  
437 validated in several studies carried out by our research group (Grant and Bacher, 2001; Grant  
438 et al., 2005, 2008), various engineering consulting firms and schools (Belanger et al., 2000;  
439 Ministère des ressources naturelles – Québec, 2002).

440

441 **Appendix B. Volumetric flow calculation (Matlab script available on request).**

442 Every node (shared vertex) within AquaDyn is represented with an X and Y Cartesian value  
443 in the grid. For each node AquaDyn provides values for three quantities: water speed in x-  
444 direction, water speed in y-direction and water depth at each time step. AquaDyn stores the  
445 results in matrices that can be programmatically retrieved and manipulated. In an AquaDyn  
446 model each element (grid cell) can be surrounded by a maximum of 3 elements and a  
447 minimum of 1 element. Boundary elements always have less than 3 surrounding elements.  
448 The exchange of water for a given element is defined in relation to each of the surrounding  
449 elements in the mesh in terms of volumetric exchange. The volumetric flow through a link  
450 from one element to another is calculated by multiplying the net velocity by the cross-  
451 sectional area through the side:

452

$$\begin{aligned} 453 \text{ Volumetric Flow} &= (\text{net velocity}) \times \text{cross-sectional area} \\ 454 &= (\text{net velocity}) \times (\text{average depth at the two nodes of the link}) \times (\text{length of link}) \end{aligned}$$

455

456 The net velocity ( $n_x \cdot u + n_y \cdot v$ ) is defined as the projection of the velocity vector ( $u, v$ ) at the  
457 centre of each side (link) into the unit perpendicular vector of the link ( $n_x, n_y$ ). The units of  
458 the velocity vector ( $u, v$ ), where  $u$  is the average velocity in the x-direction at the two ends of  
459 the link and  $v$  is similarly defined for the y direction, are adjusted to meters per day, which  
460 are compatible with Simile time steps. The unit perpendicular vector ( $n_x, n_y$ ) is defined to  
461 point towards the centre of the element (Figure B.1a). Therefore a positive/negative net  
462 velocity indicates that flow is into/out of the element.

463

464 Taking into account the node coordinates,  $(x_A, y_A)$  and  $(x_B, y_B)$ , the  $(n_x, n_y)$  vector is  
465 calculated as follows (Figure B.1a):

466

$$467 \quad n_x = -(y_A - y_B) / [(x_A - x_B)^2 + (y_A - y_B)^2]^{0.5}$$

$$468 \quad n_y = (x_A - x_B) / [(x_A - x_B)^2 + (y_A - y_B)^2]^{0.5}$$

469 or

$$470 \quad n_x = (y_A - y_B) / [(x_A - x_B)^2 + (y_A - y_B)^2]^{0.5}$$

$$471 \quad n_y = -(x_A - x_B) / [(x_A - x_B)^2 + (y_A - y_B)^2]^{0.5}$$

472

473 In order to compute which of the vectors is directed into the element, the  $(n_x, n_y)$  vector must  
474 be compared with the direction of the vector  $(p_x, p_y)$ , whose origin is the middle of the link  
475 and terminus is the opposite node (Figure B.1b). If the quantity  $n_x \cdot p_x + n_y \cdot p_y$  is positive,  $(n_x,$   
476  $n_y)$  and  $(p_x, p_y)$  follow the same direction into the element, and vice versa for negative  
477 values.

478

479 AquaDyn provides a time series for water velocity and depth at each node, and the protocol  
480 described above can be applied to each time step. However, in Simile the coupling is  
481 simplified and the Matlab script delivers to AquaDyn the volumetric water exchange as a  
482 daily average for each link following a first order upwind scheme. The error of this scheme is  
483 kept to a minimum if the spatial and temporal variation of the concentration of a conservative  
484 tracer remains small for each element and time step:

$$485 \quad \text{Error}_{spatial} (\%) = \left( \frac{|\Delta \text{Conc.}|}{\overline{\text{Conc.}}} \right)_{spatial}^2 \times 100 \quad \text{Eq. B. 1}$$

$$Error_{time} (\%) = \left( \frac{|\Delta Conc. |}{\overline{Conc.}} \right)_{time}^2 \times 100 \quad \text{Eq. B. 1}$$

486

487 where  $|\Delta Conc. |$  is the absolute difference in concentration between two connected elements at

488 a given time (Eq. B.1), or between two time steps for the same cell (Eq. B.2).  $\overline{Conc.}$  is the

489 mean concentration of both values for each case. The calculation of this error is crucial in

490 evaluating the general error of the coupling scheme.

491

492 The numerical procedure carried out to calculate the exchange and the averaging process can

493 cause a residual water imbalance within the bay. Therefore, a minimization algorithm under

494 constraint (pinv function in Matlab) was applied to the averaged exchange in order to

495 minimize the water imbalance (to make the net flows zero) while keeping the correction

496 factors as small as possible (script available on request). After this process, two CSV files are

497 created, one with the averaged volume ( $m^3$ ) of each element, the other with the averaged

498 volumetric exchange rates ( $d^{-1}$ ), *Exchange-Entry* and *Exchange-Exit*, as well as the

499 identification numbers of *Entry-Box* and *Exit-Box*, i.e. which elements are linked. This CSV

500 file contains one row for each link, i.e between every adjacent element pair and therefore

501 defines the spatial connections between them in a way interpretable by Simile.

502

503 **Appendix C. Simile structure to read spatial information (Files available on request).**

504 The use of ‘Condition’ requires variables to identify multiple instances saved in arrays inside  
505 Simile or in external CSV files. These index variables, *Entry-Box* and *Exit-Box*, are used to  
506 identify associations between elements in the grid and the calculated water volumetric  
507 exchange rates, *Exchange-Entry* and *Exchange-Exit*, to incorporate the hydrodynamics.

508

509 The following example, considering the dynamics of total suspended particulate matter  
510 (TPM, turbidity) in a bay (Figure C.1) provides a template that can be used as a core to  
511 develop any application of the coupling scheme in Simile. The ‘number of instances’ (an  
512 innate property of all submodels in Simile) of the *Bay* submodel was modified to create  $n$   
513 copies that represent the  $n$  elements of the spatial grid. Two submodels were created to  
514 manage the *Inflow* and *Outflow* of TPM and another one, *Connections*, that allows loading of  
515 external data from CSV files by using ‘Fixed Parameter’ variables. The *Connections*  
516 submodel has a ‘number of instances’ equal to the number of connections between elements,  
517 i.e. the number of rows of the external CSV file. *Inflow* and *Outflow* submodels were related  
518 with ‘Exclusive Role’ to the *Connections* submodel and ‘Normal Role’ to the *Bay* submodel.  
519 The *Inflow* and *Outflow* submodels establish if there is a connection between any two  
520 elements by means of the ‘Condition’ functions (*Cond1* and *Cond2* in Figure C.1). For  
521 example, the *Inflow* submodel checks if the *Box\_Number* variable from the *Bay* submodel  
522 matches the *Entry-Box* variable value (which depends on the rows of the external CSV file).  
523 If there is a match, the corresponding *Exit-Box* (the same row as the *Entry-Box* value) is  
524 matched with the appropriate *Box\_Number* in the *Bay* submodel. Given these prescribed  
525 connections, the flow exchange is taken from the same row of the CSV file as the data input  
526 (*Exchange-Entry* and *Exchange-Exit*). Once these exchanges are established, the physical-

527 material coupling is completed. Therefore if an element exports TPM, the appropriate mass  
528 flux of TPM (concentration \* exchange) will be removed from the TPM compartment and the  
529 same amount of TPM will be added to the element that receives the TPM. All the rows of the  
530 CSV file, exchange between elements, are processed by Simile at the same time, therefore the  
531 hydrodynamic of the whole bay is coupled simultaneously, preserving continuity in the  
532 system.

533

534 Although hydrodynamics are coupled with the biogeochemical model as described above, a  
535 fully-spatial model requires that individual variables also be initialized in space, e.g. the  
536 initial concentration of TPM in each element. Figure C.2 shows the same model with the  
537 addition of two new submodels to introduce the initial TPM value in each element. This is  
538 accomplished using an external CSV file which contains two columns, the element index  
539 variable and the initial TPM value in that element (*Box* and *Initial TPM Value*, respectively).  
540 The submodel called *Initial TPM* reads these variables from an external CSV file using  
541 ‘Fixed Parameter’ variables. The submodel called *Initial Condition* checks if the  
542 *Box\_Number* variable from the *Bay* submodel matches the *Box* variable value from the *Initial*  
543 *TPM* submodel (which depends on the rows of the external CSV file). If there is a match the  
544 *Initial TPM Value* will be introduced into the *Bay* submodel as the initial value of TPM for  
545 the *Box\_Number* element. The same procedure can be applied to other variables, such as the  
546 presence/absence of aquaculture, providing a very fine spatial resolution of the initial  
547 conditions.

548 **References**

- 549 Allen, J.I., Aiken, J., Anderson, T.R., Buitenhuis, E., Cornell, S., Geider, R.J., Haines, K.,  
550 Hirata, T., Holt, J., Le Quere, C., Hardman-Mountford, N., Ross, O.N., Sinha, B., While, J.,  
551 2010. Marine ecosystem models for earth system applications: The MarQUEST experience.  
552 *J. Marine. Syst.* 81, 19-33.
- 553
- 554 Bacher, C., Duarte, P., Ferreira, J.G., Héral, M., Raillard, O., 1998. Assessment and  
555 comparison of the Marennes-Oléron Bay (France) and Carlingford Lough (Ireland) Carrying  
556 Capacity with ecosystem models. *Aquat. Ecol.* 31, 379-394.
- 557
- 558 Bacher, C., Grant, J., Hawkins, A., Fang, J., Zhu, P., Duarte, P., 2003. Modelling the effect of  
559 food depletion on scallop growth in Sungo Bay (China). *Aquat. Living. Resour.* 16, 10-24.
- 560
- 561 Baretta, J.W., Ebenhoh, H., Ruardij, P., 1995. The European-regional-seas-ecosystem-model,  
562 a complex marine ecosystem model. *Neth. J. Sea. Res.* 33, 233-246.
- 563
- 564 Behm, P., Boumans, R.M.J., Short, F.T., 2004. Spatial modeling of eelgrass distribution in  
565 Great Bay, New Hampshire, in: Constanza, R., Voinov, A. (Eds.), *Landscape simulation*  
566 *modelling. A spatially explicit, dynamic approach.* Springer-Verlag, New York, pp. 173-196.
- 567
- 568 Belanger, M., Carreau, M., Vincent, A. 2000. A test field calibration to validate shallow-  
569 water codes: the case of the Ste- Marguerite River with AquaDyn. Centre de Recherche en  
570 Calcul Applique (CERCA) Technical Report TR-2006-01, University of Montreal.
- 571



572 Chapelle, A., Lazure, P., Menesguen, A., 1994. Modeling eutrophication events in a coastal  
573 ecosystem – sensitivity analysis. *Estuarine Coast. Shelf Sci.* 39, 529-548.

574

575 Chapelle, A., Menesguen, A., Deslous-Paoli, J.M., Souchu, P., Mazouni, N., Vaquer, A.,  
576 Millet, B., 2000. Modelling nitrogen, primary production and oxygen in a Mediterranean  
577 lagoon. Impact of oysters farming and inputs from the watershed. *Ecol. Model.* 127, 161-181.

578

579 Cloern, J.E., 1982. Does the benthos control phytoplankton bio- mass in southern San  
580 Francisco Bay? *Mar. Ecol. Prog. Ser.* 9, 191–202.

581

582 Cranford, P.J., Strain, P.M., Dowd, M., Hargrave, B.T., Grant, J., Archambault, M.C., 2007.  
583 Influence of mussel aquaculture on nitrogen dynamics in a nutrient enriched coastal  
584 embayment. *Mar. Ecol. Prog. Ser.* 347, 61-78.

585

586 Dowd, M., 1997. On predicting the growth of cultured bivalves. *Ecol. Model.* 104, 113-131.

587

588 Dowd, M., 2003. Seston dynamics in a tidal inlet with shellfish aquaculture: a model study  
589 using tracer equations. *Estuarine Coast. Shelf Sci.* 57, 523-537.

590

591 Dowd, M., 2005. A bio-physical coastal ecosystem model for assessing environmental effects  
592 of marine bivalve aquaculture. *Ecol. Model.* 183, 323-346.

593

594 Duarte, P., Meneses, R., Hawkins, A.J.S., Zhu, M., Fang, J., Grant, J., 2003. Mathematical  
595 modelling to assess the carrying capacity for multi-species culture within coastal waters.  
596 *Ecol. Model.* 168, 109-143.  
597

598 Elshorbagy, A., Teegavarapu, R.S.V., Ormsbee, L., 2006. Assessment of pathogen pollution  
599 in watersheds using object-oriented modeling and probabilistic analysis. *J. Hydroinform.* 8,  
600 51-63.  
601

602 Fennel, W., Neumann, T., 2004. Introduction to the modelling of marine ecosystems.  
603 Elsevier Oceanography Series, 72. Elsevier, Amsterdam.  
604

605 Fennel, K., Wilkin, J., Levin, J., Moisan, J., O'Reilly, J., Haidvogel, D., 2006. Nitrogen  
606 cycling in the Middle Atlantic Bight: Results from a three-dimensional model and  
607 implications for the North Atlantic nitrogen budget. *Glob. Biogeochem. Cycles* 20, GB3007,  
608 doi:10.1029/2005GB002456.  
609

610 Ferreira, J., Duarte, P., Ball, B., 1998. Trophic capacity of Carlingford Lough for aquaculture  
611 - analysis by ecological modelling. *Aquat. Ecol.* 31, 361-379.  
612

613 Ferreira, J.G., Hawkins, A.J.S., Monteiro, P., Moore, H., Service, M., Pascoe, P.L., Ramos,  
614 L., Sequeira, A., 2008. Integrated assessment of ecosystem-scale carrying capacity in shellfish  
615 growing areas. *Aquaculture* 275, 138-151.  
616

617 Filgueira, R., Grant, J., 2009. A box model for ecosystem-level management of mussel  
618 culture carrying capacity in a coastal bay. *Ecosystems* 12, 1222-1233.

619

620 Filgueira, R., Grant, J., Strand, Ø., Asplin, L., Aure, J., 2010. A simulation model of carrying  
621 capacity for mussel culture in a Norwegian fjord: role of forced upwelling. *Aquaculture* 308,  
622 20-27.

623

624 Grant, J., Bacher, C., Cranford, P.J., Guyondet, T., Carreau, M., 2008. A spatially explicit  
625 ecosystem model of seston depletion in dense mussel culture. *J. Mar. Syst.* 73, 155-168.

626

627 Grant, J., Bugden, G., Horne, E., Archambault, M.-C., Carreau, M., 2007b. Remote sensing  
628 of particle depletion by coastal suspension-feeders. *Can. J. Fish. Aquat. Sci.* 64, 387-390.

629

630 Grant, J., Cranford, P., Hargrave, B., Carreau, M., Schofield, B., Armsworthy, S., Buerdett-  
631 Coutts, V., Ibarra, D., 2005. A model of aquaculture biodeposition for multiple estuaries and  
632 field validation at blue mussel (*Mytilus edulis*) culture sites in eastern Canada. *Can. J. Fish.*  
633 *Aquat. Sci.* 62, 1271-1285.

634

635 Grant, J., Curran, K.J., Guyondet, T.L., Tita, G., Bacher, C., Koutitonsky, V., Dowd, M.,  
636 2007a. A box model of carrying capacity for suspended mussel aquaculture in Lagune de la  
637 Grande-Entrée, îles-de-la-Madeleine, Québec. *Ecol. Model.* 200, 193-206.

638

639 Grant, J., Dowd, M., Thompson, K., Emerson, C., Hatcher, A., 1993. Perspectives on field  
640 studies and related biological models of bivalve growth, in: Dame, R. (Ed.), Bivalve filter  
641 feeders and marine ecosystem processes. Springer, New York, pp. 371-420.  
642

643 Grant, J., Filgueira, R., (in press). The application of dynamic modelling to prediction of  
644 production carrying capacity in shellfish farming, in: Shumway, S (Ed.), Shellfish  
645 aquaculture and the environment. John Wiley & Sons, New York.  
646

647 Héral, M., 1993. Why carrying capacity models are useful tools for management of bivalve  
648 molluscs culture, in: Dame, R. (Ed.), Bivalve filter-feeders in estuarine and coastal  
649 ecosystems. NATO ASI Series, pp. 455-477.  
650

651 Kjerfve, B., Magill, K.E., 1989. Geographic and hydrodynamic characteristics of shallow  
652 coastal lagoons. Mar. Geol. 88, 187-199.  
653

654 Kremer, J., Nixon, S.W., 1978. A Coastal Marine Ecosystem: Simulation and Analysis.  
655 Springer-Verlag, New York.  
656

657 Maxwell, T., Constanza, R., 1994. Spatial ecosystem modelling in a distributed  
658 computational environment, in: van den Bergh, J., van der Straaten, J. (Eds.), Towards  
659 Sustainable Development: Concepts, Methods, and Policy. Island Press, Washington DC.  
660

661 Maxwell, T., Constanza, R., 1995. Distributed modular spatial ecosystem modelling.  
662 International Journal of Computer Simulation 5, 247-262.

663

664 Maxwell, T., Constanza, R., 1997a. An open geographic modelling environment. *Simulation*  
665 *Journal* 68, 175-185.

666

667 Maxwell, T., Constanza, R., 1997b. A language for modular spatio-temporal simulation.  
668 *Ecol. Model.* 103, 105-113.

669

670 Ministère des ressources naturelles – Québec, 2002. Régularisation des crues du bassin versant  
671 du lac Kénogami. Saguenay-Lac-Saint-Jean 621 1-01-005

672

673 Muetzelfeldt, R., Massheder, J., 2003. The Simile visual modelling environment. *Eur. J.*  
674 *Agron.* 18, 345-358.

675

676 North, E.W., King, D.M., Xu, J., Hood, R.R., Newell, R.I.E., Paynter, K., Kellogg, M.L.,  
677 Liddel, M.K., Boesch, D.F., 2010. Linking optimization and ecological models in a decision  
678 support tool for oyster restoration and management. *Ecol. Appl.* 20, 851-866.

679

680 Pastres, R., Solidoro, C., Cossarini, G., Canu, D.M., Dejak, C., 2001. Managing the rearing of  
681 *Tapes philippinarum* in the lagoon of Venice: a decision support system. *Ecol. Model.* 138,  
682 231-245.

683

684 Pereira, A., Duarte, P., 2005. EcoDynamo: Ecological Dynamics Model Application. DITTY  
685 Report. Available at <http://www.dittyproject.org/Reports.asp>

686

687 Pereira, A., Duarte, P., Norro, A., 2006. Different modelling tools of aquatic ecosystems: A  
688 proposal for a unified approach. *Ecol. Inform.* 1, 407-421.

689

690 Raillard, O., Ménesguen, A., 1994. An ecosystem model for the estimating the carrying  
691 capacity of a macrotidal shellfish system. *Mar. Ecol. Prog. Ser.* 115, 117-130.

692

693 Randhir, T.O., Tsvetkova, O., 2011. Spatiotemporal dynamics of landscape pattern and  
694 hydrologic process in watershed systems. *J. Hydrol.* 404, 1-12.

695

696 Sarmiento, J.L., Slater, R.D., Fashman, M.J.R., Ducklow, H.W., Toggweiler, J.R., Evans,  
697 G.T., 1993. A seasonal 3-dimensional ecosystem model of nitrogen cycling in the North-  
698 Atlantic euphotic zone. *Global Biochem. Cy.* 7, 417-450.

699

700 Shchepetkin, A.F., McWilliams, J.C., 2005. The Regional Ocean Modelling SystemL A split-  
701 explicit, free-surface, topography following coordinates ocean model. *Ocean Model.* 9, 347-  
702 404.

703

704 Silvert, W., 1993. Object-oriented ecosystem modeling. *Ecol. Model.* 68, 91-118.

705

706 Spillman, C.M., Hamilton, D.P., Hipsey, M.R., Imberger, J., 2008. A spatially resolved  
707 model of seasonal variations in phytoplankton and clam (*Tapes philippinarum*) biomass in  
708 Barbamarco Lagoon, Italy. *Estuarine Coast. Shelf Sci.* 79, 187-203.

709

710 Umgiesser, G., Canu, D.M., Solidoro, C., Ambrose, R., 2003. A finite element ecological  
711 model: a first application to the Venice Lagoon. *Environ. Modell. Softw.* 18, 131-145.  
712

713 Waite, L., Grant, J., Davidson, J., 2005. Bay-scale spatial growth variation of mussels *Mytilus*  
714 *edulis* in suspended culture, Prince Edward Island, Canada. *Mar. Ecol. Prog. Ser.* 297, 157-  
715 167.  
716

717 Walker, T.R., Grant, J., 2009. Quantifying erosion rates and stability of bottom sediments at  
718 mussel aquaculture sites in Prince Edward Island. *J. Marine. Syst.* 75, 46-55.  
719

720 Zar, J.H., 1984. *Biostatistical Analysis*. New Jersey: Prentice-Hall.  
721

722 **Figure Legends**

723 **Figure 1.** Triangular unstructured finite grid example. A. Structure and nomenclature of the  
724 components of the grip. B. Additional points calculated to plot Simile results in GIS software.

725

726 **Figure 2.** Coupling scheme developed for Tracadie Bay: triangular finite grid created in  
727 AquaDyn, example of water exchange file delivered by Matlab and description of the  
728 structure developed in Simile, which combines the biogeochemical model and the submodel  
729 that reads the spatial topology and executes the hydrodynamics.

730

731 **Figure 3.** Study area. A. Tracadie Bay (Prince Edward Island, Canada). B. Triangular  
732 unstructured grid of Tracadie Bay created in AquaDyn. The circle represents Node # 236,  
733 where the current-meter was deployed, and the two coloured elements are Element # 182  
734 (South) and # 385 (North), where the conservative tracer verifications were performed.

735

736 **Figure 4.** Conservative tracer concentration (units  $\text{m}^{-3}$ ) in Tracadie Bay after 10 days in  
737 AquaDyn and Simile.

738

739 **Figure 5.** Time series of conservative tracer concentration (units  $\text{m}^{-3}$ ) in Element # 182 and #  
740 385 in AquaDyn and Simile.

741

742 **Figure 6.** Bay averaged time series of chlorophyll depletion (%) in both 1998 and 1999.  
743 Continuous line represents the average value and dotted lines the standard deviation.

744

745 **Figure 7.** Time averaged percentage of chlorophyll depletion (%) in both 1998 and 1999.



746

747 **Figure B.1.** Structure of the element defined by the nodes A ( $x_A, y_A$ ), B ( $x_B, y_B$ ) and C  
748 ( $x_C, y_C$ ) and vectors used to calculate the flow through the link A-B. A. Perpendicular vector  
749 ( $n_x, n_y$ ) to the link A-B. B. Vector ( $p_x, p_y$ ) which origin in the middle of the link A-B, D  
750 ( $x_D, y_D$ ), and directed to the opposite node of A-B, C ( $x_C, y_C$ ).

751

752 **Figure C.1.** Simile model of a bay in which only the TPM is considered. *Inflow*, *Outflow* and  
753 *Connections* submodels provide the information to couple AquaDyn to Simile. The submodel  
754 called *Submodel – Legend* describes the different symbols used in the model according to the  
755 nomenclature used in Simile (Muetzelfeldt and Massheder 2003).

756

757 **Figure C.2.** Simile model with a submodel to establish initial values at the beginning of the  
758 simulation.

Figure 1  
[Click here to download high resolution image](#)

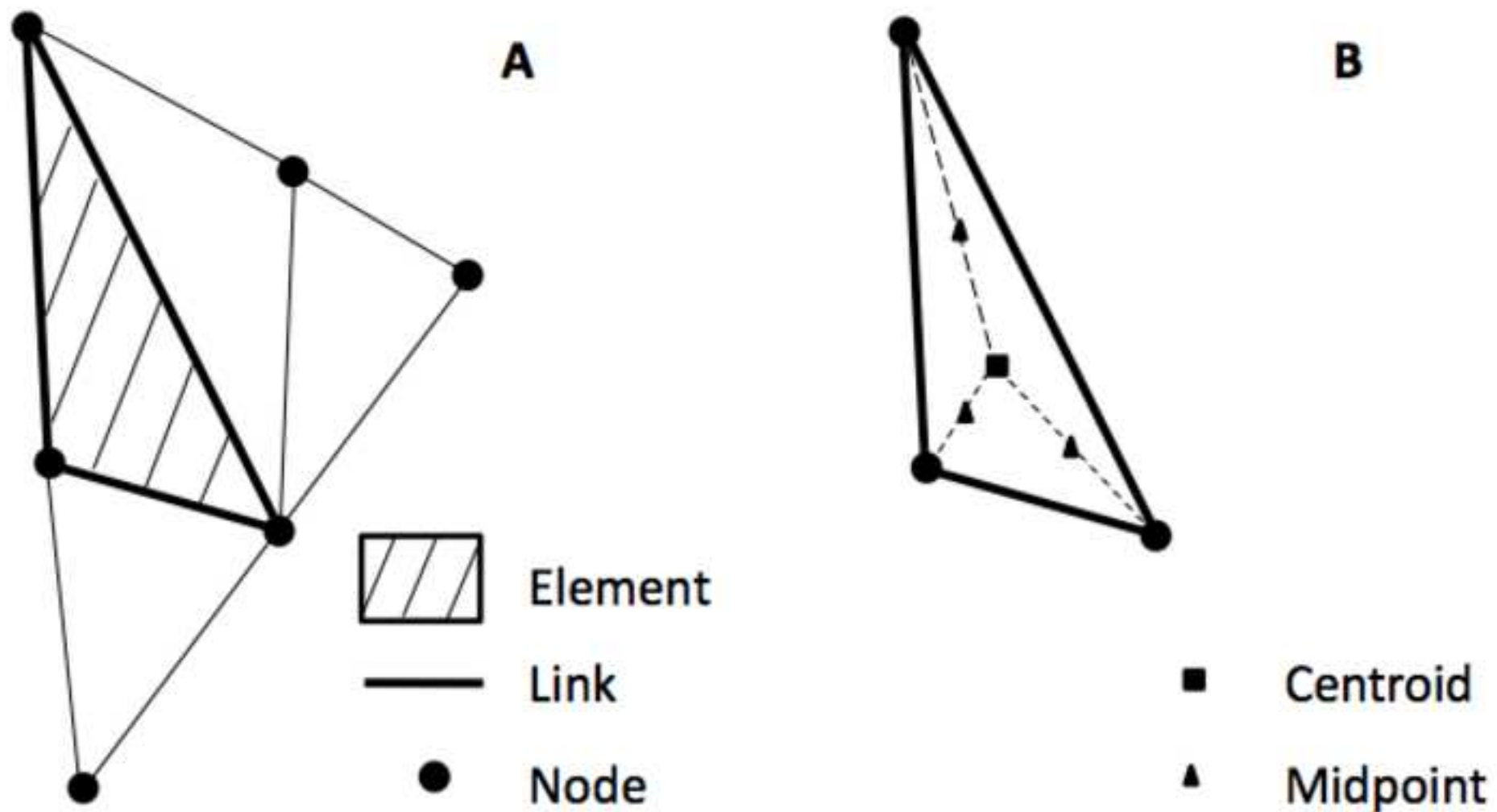


Figure 2  
[Click here to download high resolution image](#)

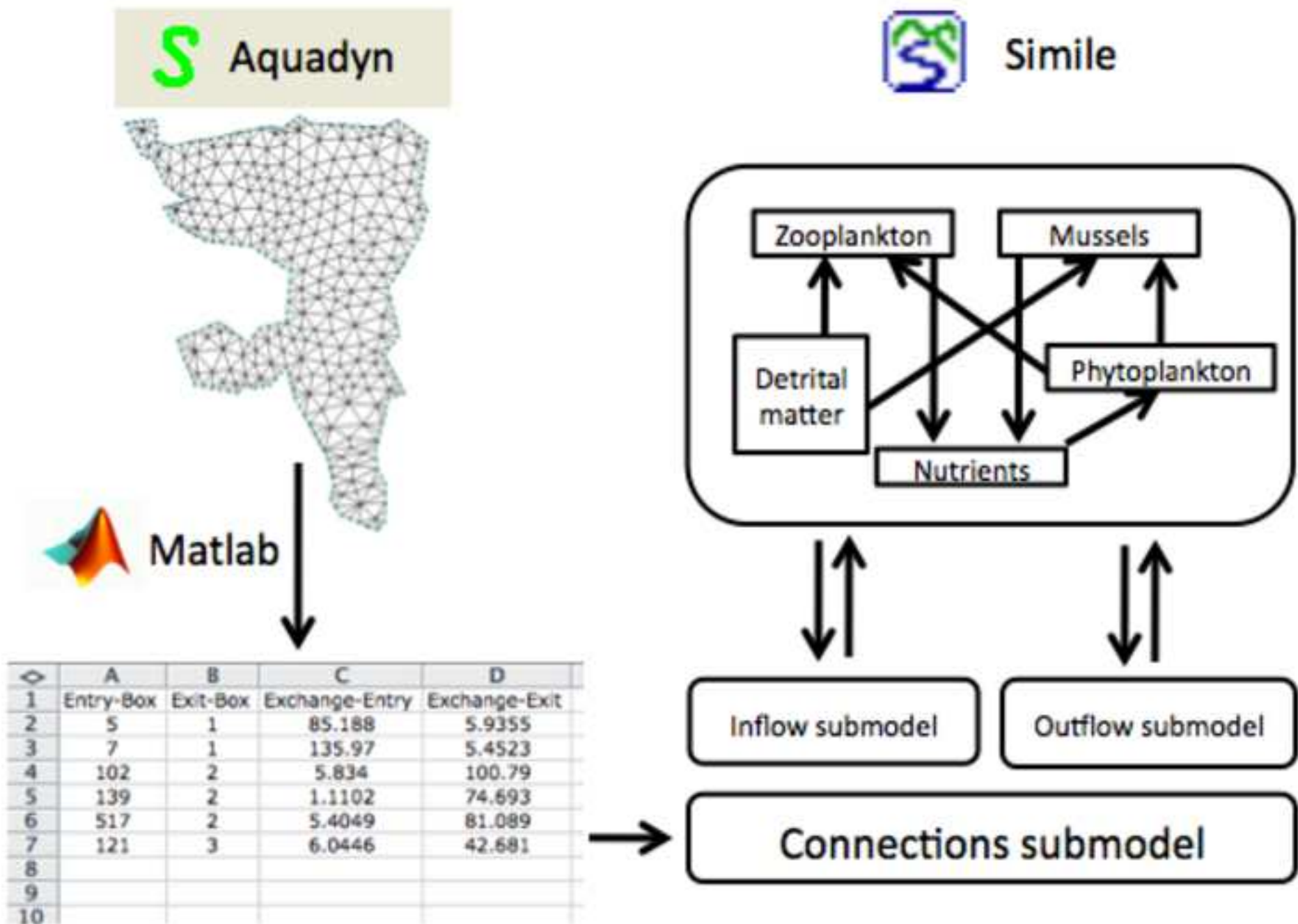


Figure 3  
[Click here to download high resolution image](#)

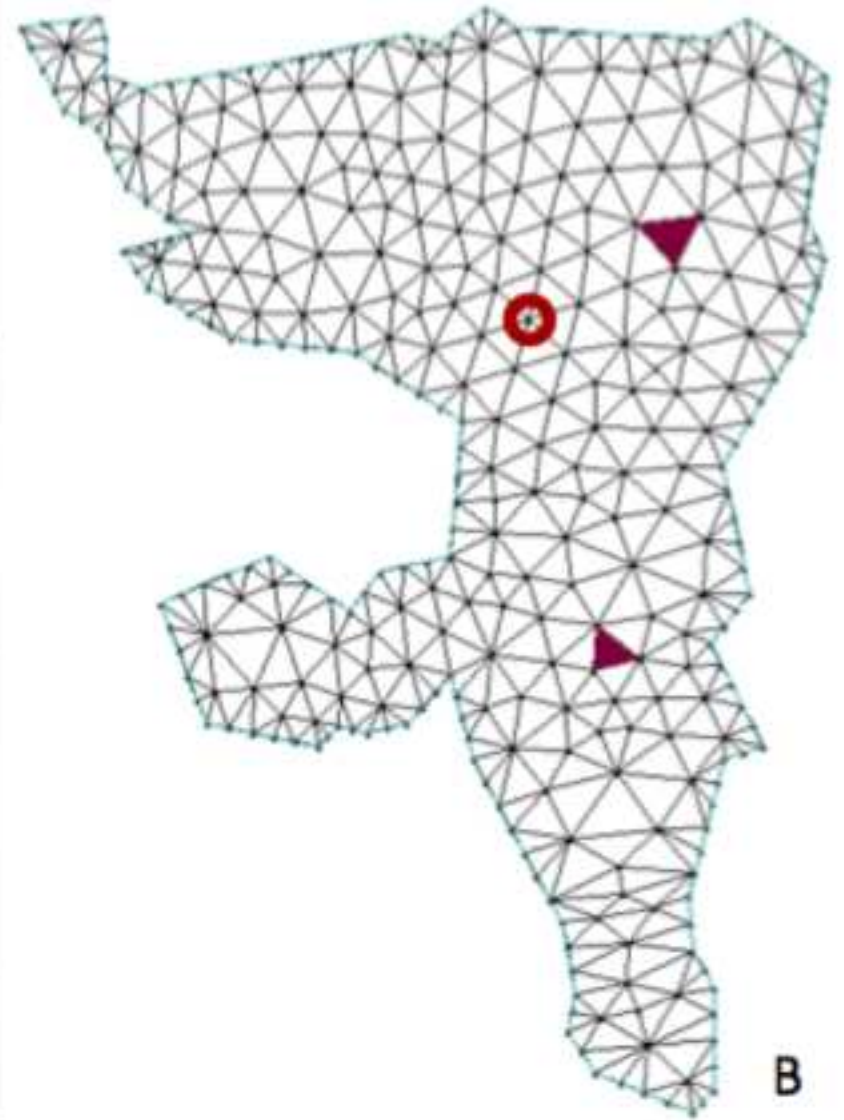
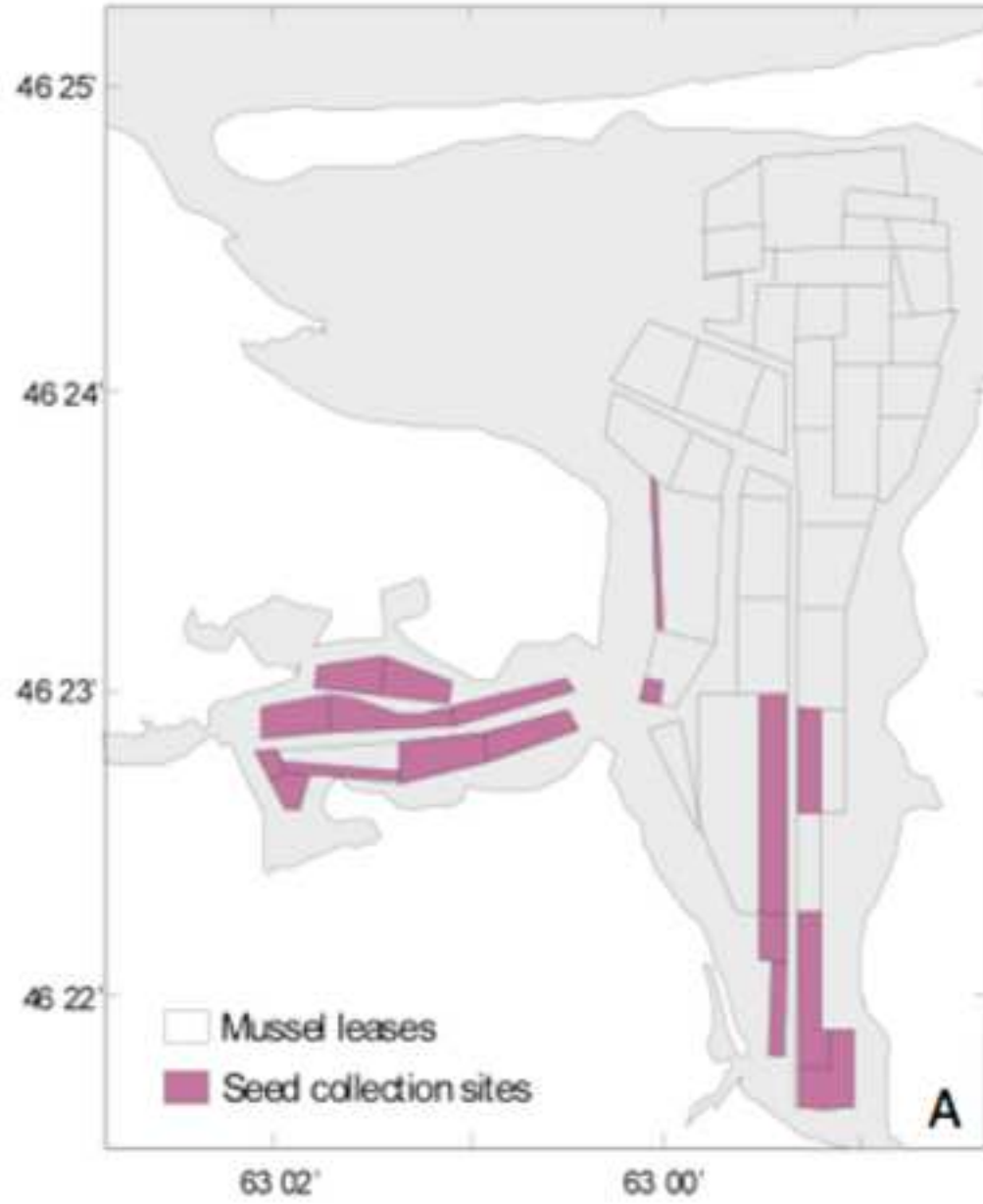


Figure 4  
[Click here to download high resolution image](#)

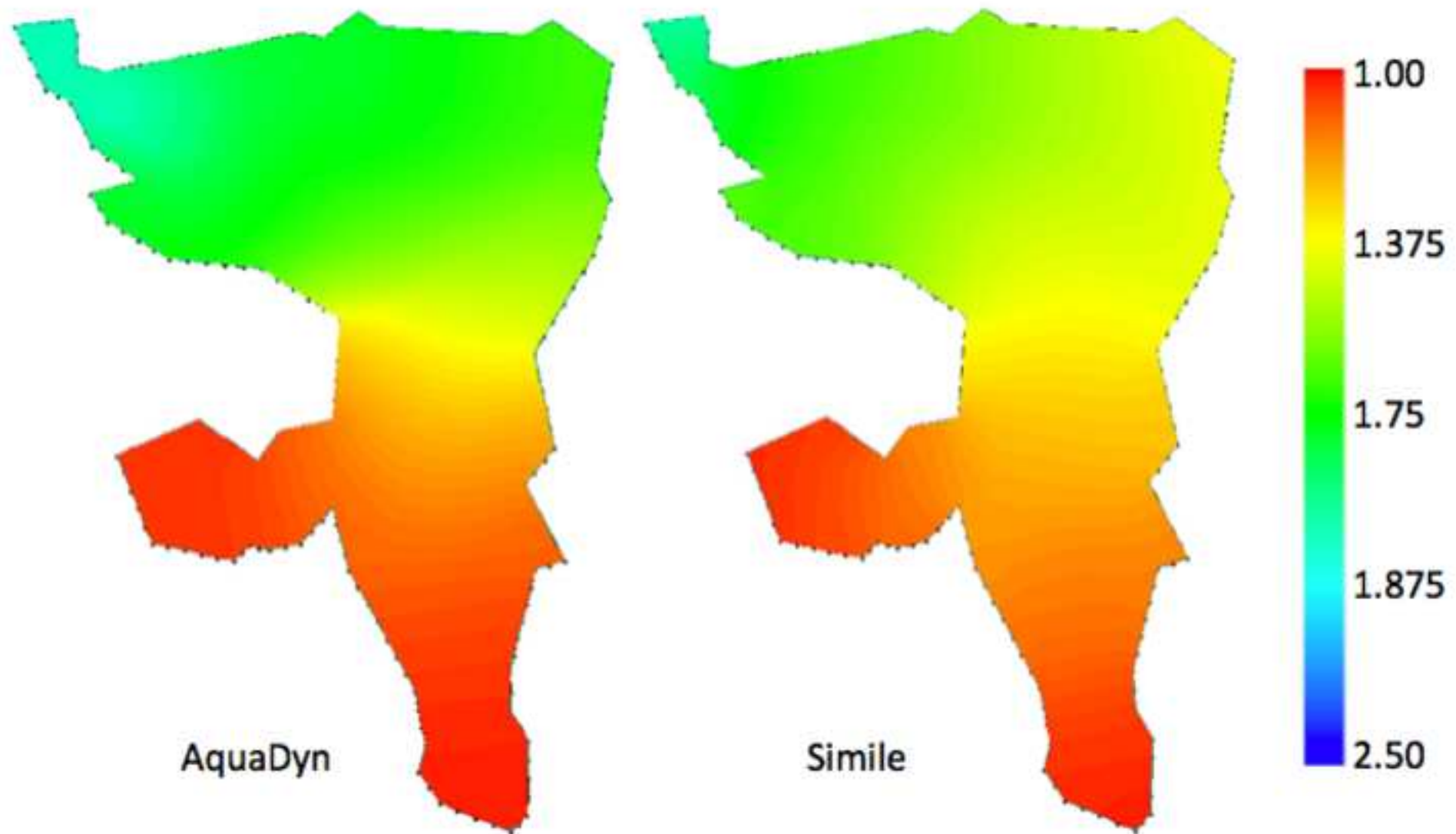


Figure 5  
[Click here to download high resolution image](#)

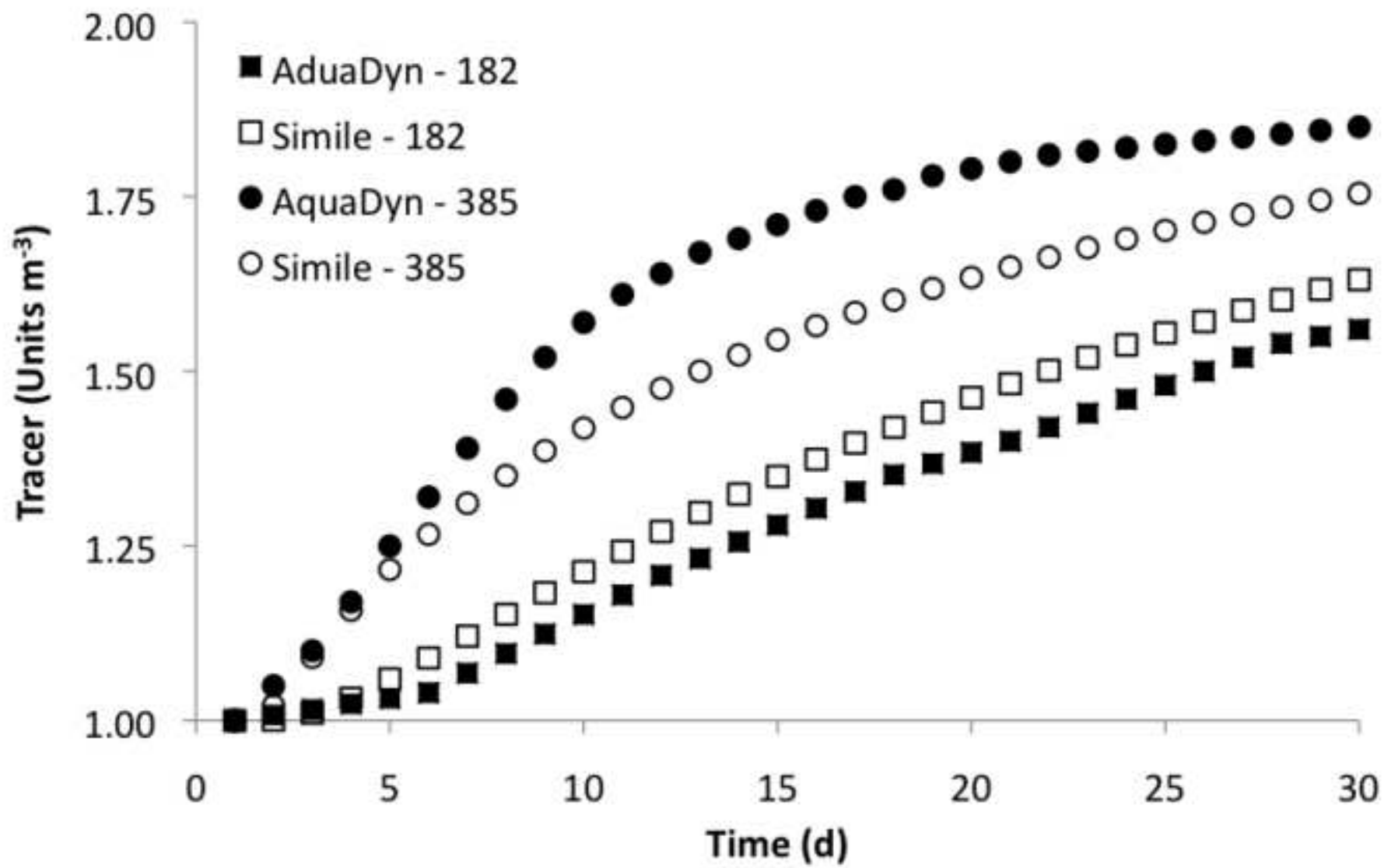


Figure 6  
[Click here to download high resolution image](#)

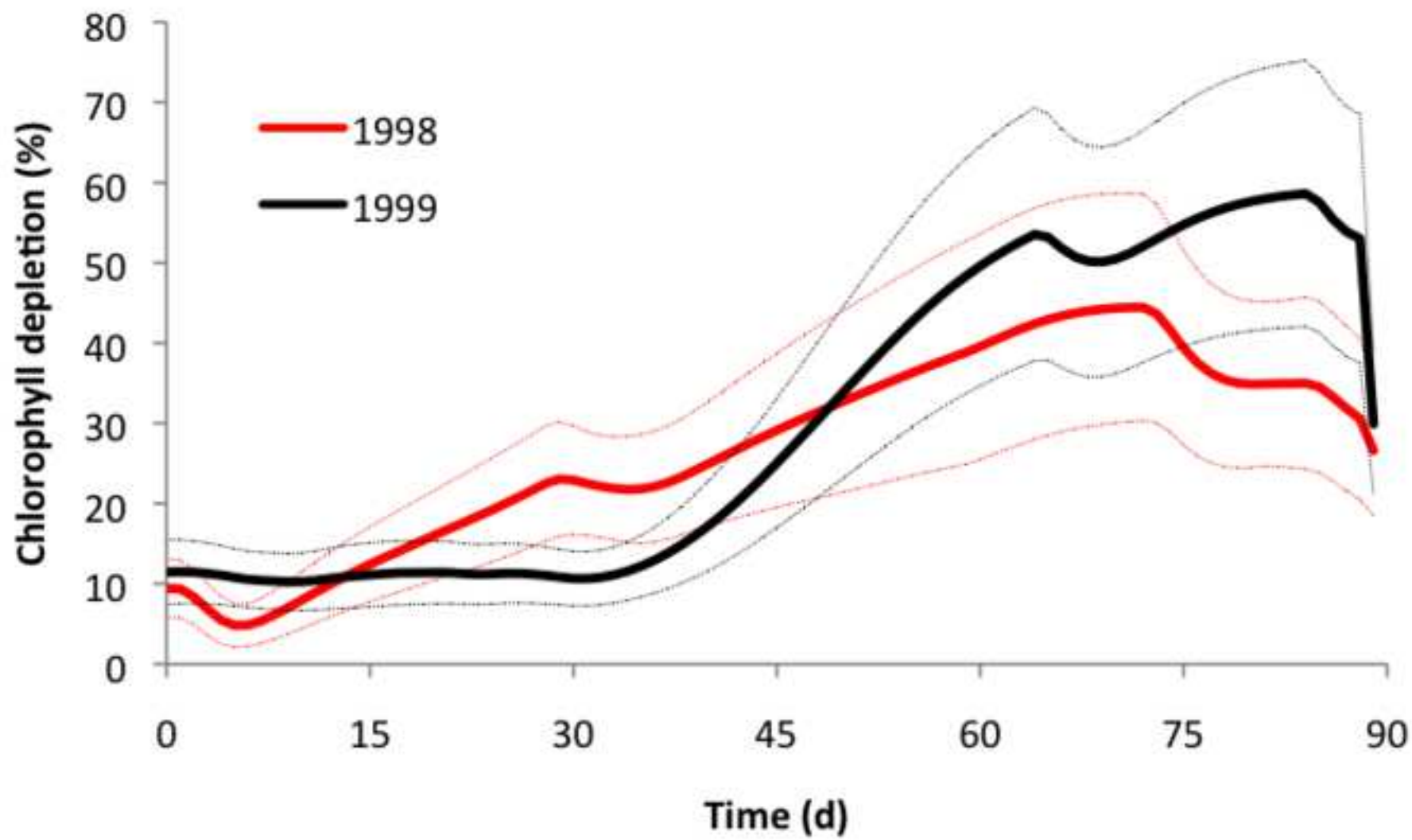




Figure 7  
[Click here to download high resolution image](#)

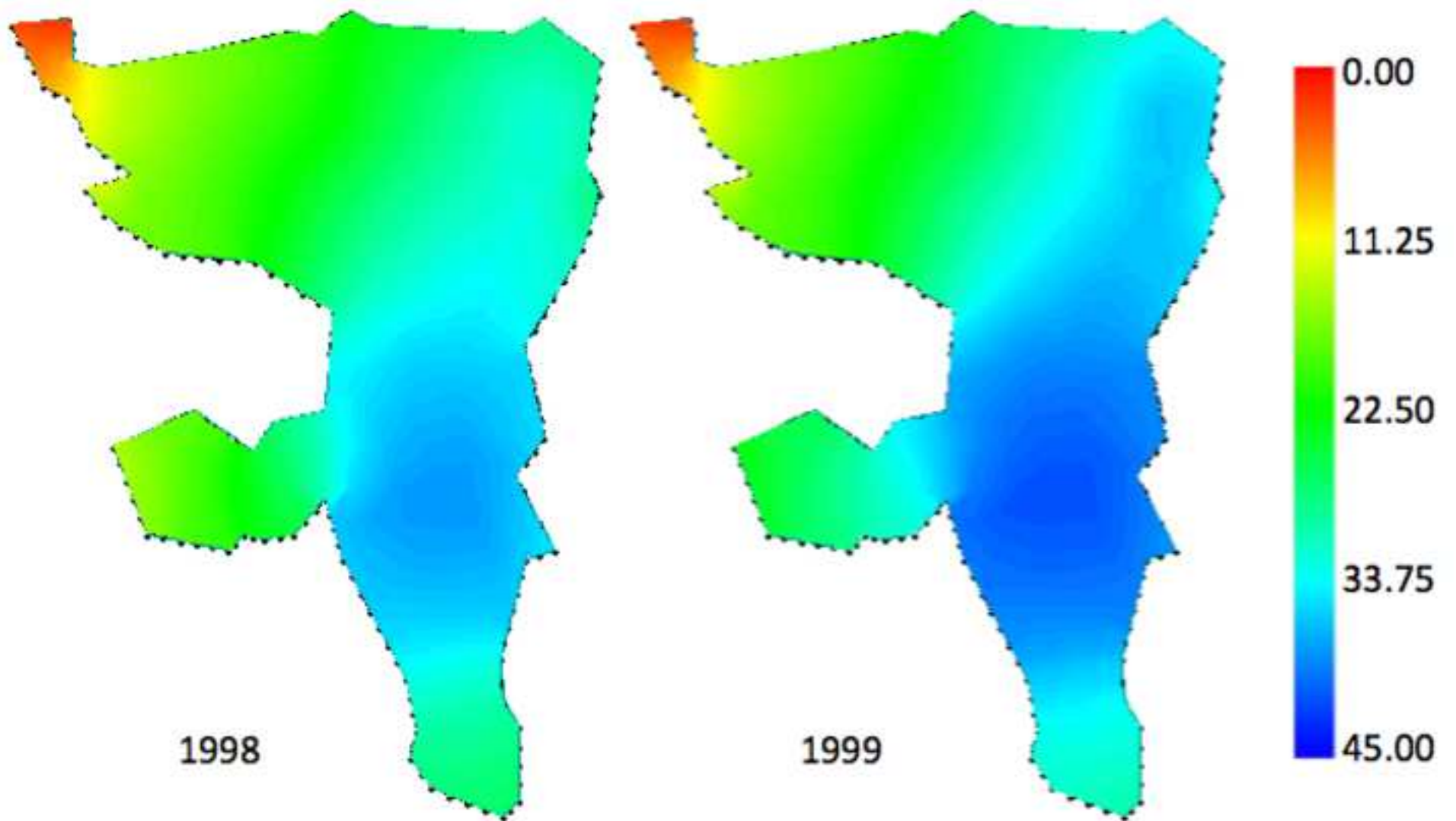




Figure B-1  
[Click here to download high resolution image](#)

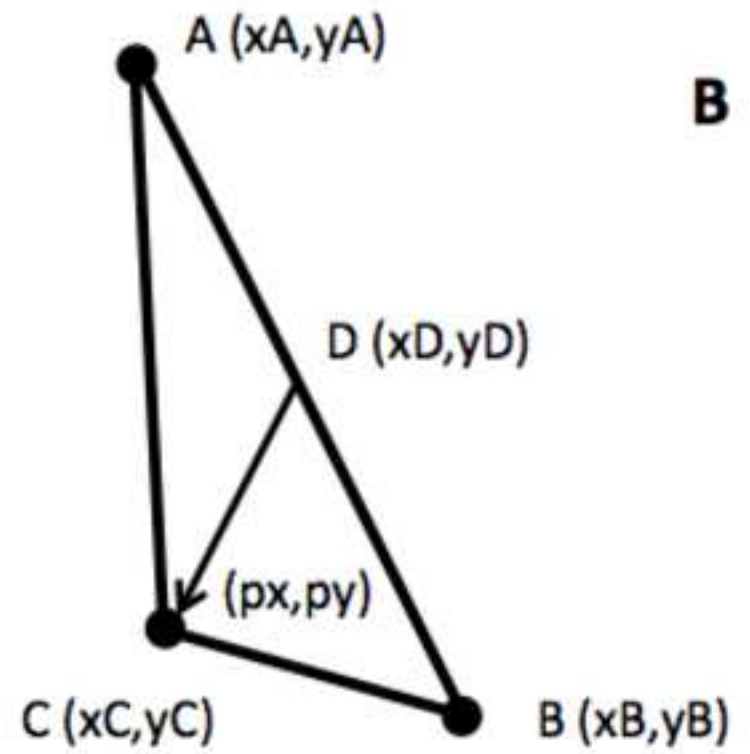
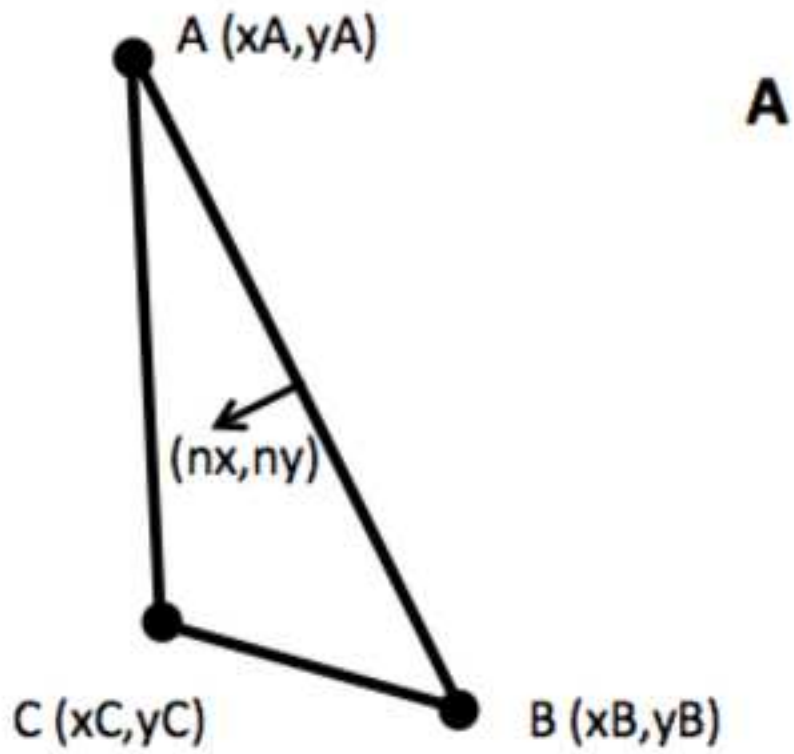


Figure C-1  
[Click here to download high resolution image](#)

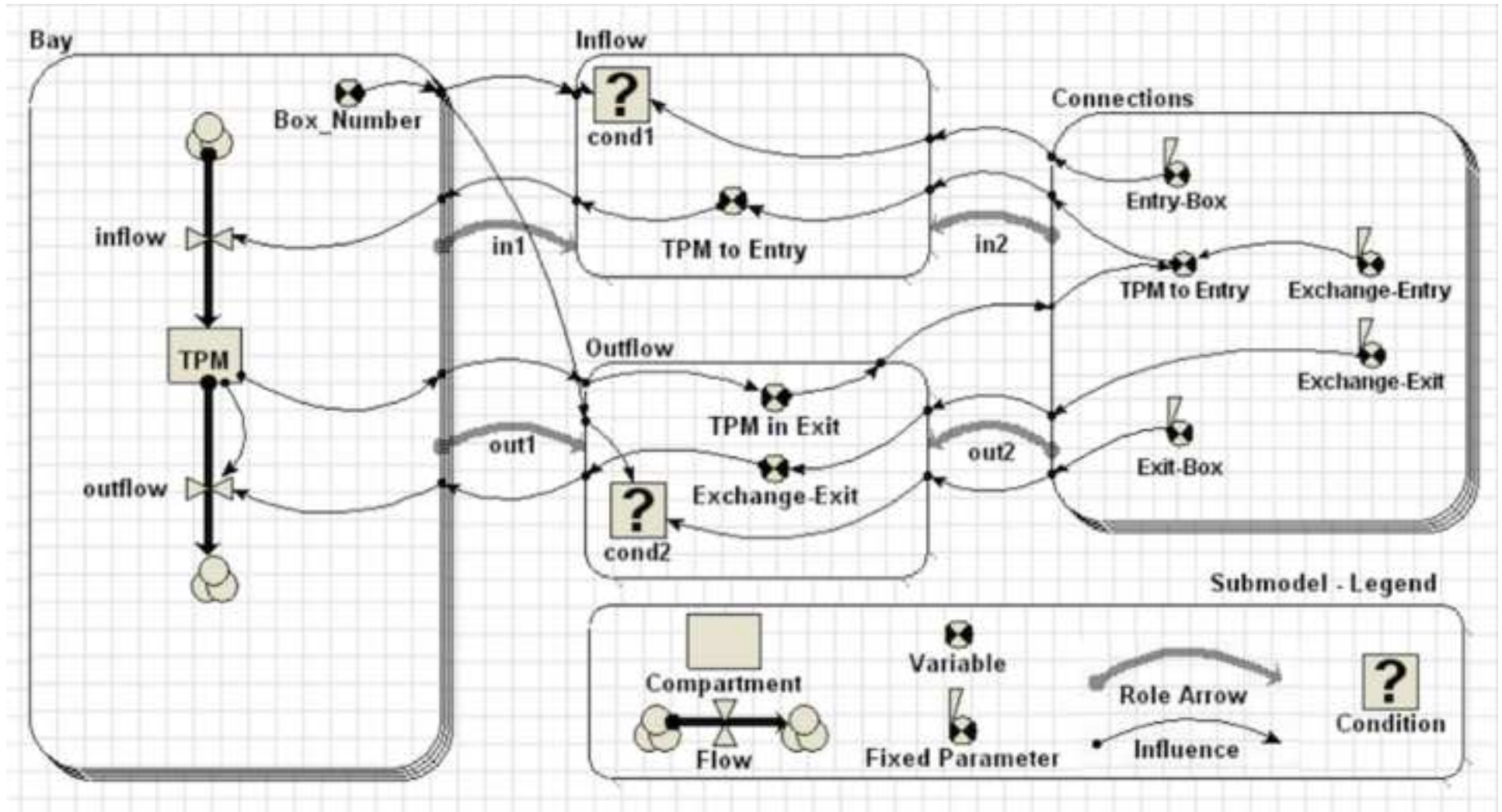
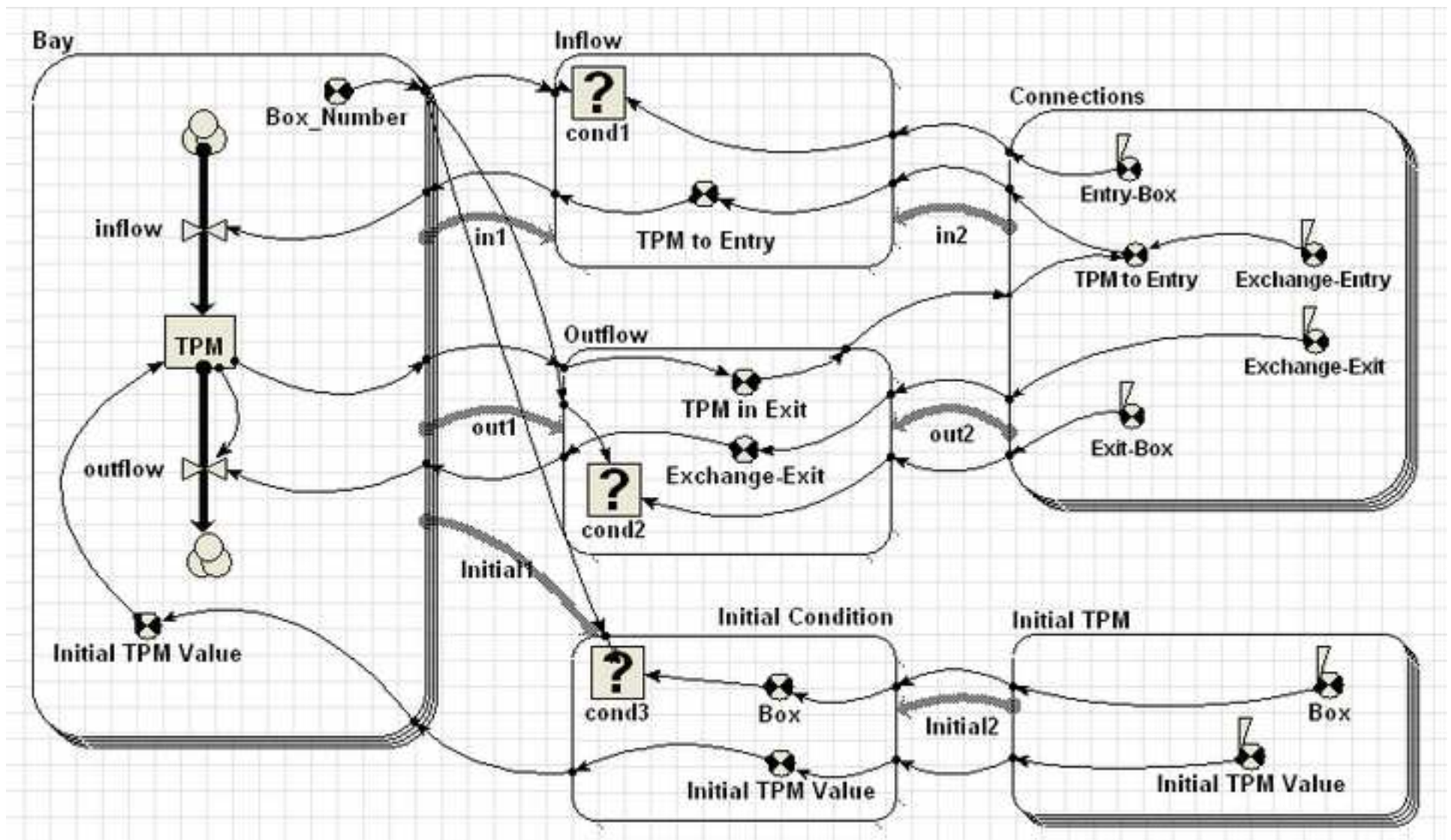


Figure C-2  
[Click here to download high resolution image](#)



**Table 1.** General model equations and description.

<b>Term</b>	<b>Definition</b>	<b>Reference</b>
$dP/dt$	Phytoplankton change rate ( $\text{mgC m}^{-3} \text{d}^{-1}$ )	
$P_{\text{growth}}$	Phytoplankton growth	
$P_{\text{mortality}}$	Phytoplankton mortality	
$M_{\text{grazing}}$	Mussel grazing on phytoplankton	Eq. 7 in Grant et al. (2007)
$P_{\text{mixing}}$	Exchange of phytoplankton with adjacent elements and far field	
$dN/dt$	Nitrogen change rate ( $\text{mgN m}^{-3} \text{d}^{-1}$ )	
$N_{\text{river}}$	Nitrogen river discharge	River discharge x River Nitrogen concentration
$M_{\text{excretion}}$	Mussel nitrogen excretion	Eq. 17 in Grant et al. (2007)
$P_{\text{uptake}}$	Phytoplankton nitrogen uptake	
$N_{\text{mixing}}$	Exchange of nitrogen with adjacent elements and far field	Eq. 15 in Grant et al. (2007)
$dD/dt$	Detritus change rate ( $\text{mgC m}^{-3} \text{d}^{-1}$ )	
$D_{\text{resuspension}}$	Detritus resuspension forced by wind	See Filgueira and Grant (2009)
$M_{\text{feces}}$	Mussel feces production	Eq. 5 in Grant et al. (2007)
$P_{\text{mortality}}$	Phytoplankton mortality	See above
$D_{\text{sinking}}$	Detritus removal by sinking	
$M_{\text{grazing}}$	Mussel grazing on detrital matter	Eq. 5 in Grant et al. (2007)
$D_{\text{mixing}}$	Exchange of detritus with adjacent elements and far field	
$dM/dt$	Mussel change rate ( $\text{mgC m}^{-3} \text{d}^{-1}$ )	
$M_{\text{net growth}}$	Mussel net growth	Eq. 1 in Grant et al. (2007)
$M_{\text{seeding}}$	Income of mussel biomass by seeding	These rates are not calculated, their sum is assumed to
$M_{\text{mortality}}$	Mussel natural mortality	compensate $M_{\text{net growth}}$
$M_{\text{harvesting}}$	Mussel mortality by harvesting	

**Table 2.** Analysis of velocity modulus measured with the current meter (46°23'56''N, 62°59'56''W) and the closest node in AquaDyn model, Node # 236. Values are in  $\text{cm s}^{-1}$ .

	<b>Current Meter</b>	<b>AquaDyn</b>
Maximum	21.57	7.66
Minimum	0.18	0.09
Mean	5.09	3.67
Standard Dev.	2.93	1.35
Median	4.48	4.18

**Table 3.** Summary of different modelling environments, most relevant characteristics, classification of coupling and references.

<b>Modelling environment</b>	<b>Characteristics</b>	<b>Coupling</b>	<b>References / Examples</b>
<i>General modelling environments</i>			
Spatial Modelling Environment	Object oriented simulation environment Specific programming language Possibility to be coupled to other software	Integration / Offline	Maxwell and Constanza, 1994, 1995, 1997a, 1997b
Matlab / Fortran	Programming language High flexibility and mathematical power Possibility to be coupled to other software	Integration / Offline / Online	Fennel and Neumann, 2004 Umgiesser et al., 2003
GEMSS / ROMS	Physical modelling environment Possibility to use pre-generated, but usually non-modifiable biological models	Online	Fennel et al., 2006
<i>Aquaculture examples</i>			
Not specified	Improve economic yield of <i>Tapes philippinarum</i> culture (Venice Lagoon)	Not specified	Pastres et al., 2001
EcoDynamo	Simulate physical, biogeochemical and anthropogenic processes in aquatic ecosystems Possibility to be coupled to other software	Offline	Pereira et al. 2006
EcoWin2000 /Delft3D-Flow / ShellSIM	EcoWin2000 is a platform for integration of different submodels or software Evaluate carrying capacity for aquaculture (Northern Ireland)	Offline	Ferreira et al., 2008
Matlab - AquaDyn	Evaluate bivalve grazing activity (Tracadie Bay)	Offline	Grant et al., 2008
ELCOM / CAEDYM	Elucidate temporal and spatial variability of food supply to clams (Barbamarco Lagoon)	Offline	Spillman et al., 2008

GEMMS (Generalized Environmental Modelling System for Surfacewaters), ROMS (Regional Ocean Modelling System), ELCOM (Estuary and Lake Computer Model), CAEDYM (Computational Aquatic Ecosystem Dynamic Model), EcoDynamo (Ecological Dynamic Model).